Sol-Gel Synthesis, Crystalline Size, Dislocation Density and Microstrain of $LiNi_{0.85}Co_{0.10}Mn_{0.05}O_2$ Cathode Material for Lithium-ion Batteries

Monika[a)], Ashish Kumar Mishra[b)], Balbir Singh Patial[c,*]

Department of Physics, Himachal Pradesh University, Summerhill, Shimla, Himachal Pradesh-171005, India

[a)] monika2019panghal@gmail.com

[b)] ashgarg32150@gmail.com

[c)] bspatial@gmail.com, bspatial@hpuniv.ac.in

Abstract

Lithium-ion batteries (LIBs) are essential energy storage solutions for a wide range of applications. The cathode material significantly influences the performance of LIBs. Nickel-cobalt-manganese (NCM) ternary cathode materials have gained prominence due to their potential to offer high capacity, stability and voltage characteristics. In this paper, we focus on the synthesis of NCM cathode material using sol-gel method and its characterization primarily through X-ray diffraction (XRD) analysis. The crystal structure of the synthesized material is investigated using XRD. These XRD patterns are analyzed to estimate particle size and to deduce crystalline size, dislocation density and microstrain. This study helps us better understand how NCM materials are put together, which is important for making high performance lithium-ion batteries. These batteries are used in laptops, electric cars, etc.

Keywords: Lithium-ion batteries, cathode material, NCM ternary cathode, sol-gel synthesis, X-ray diffraction.

*** Address of correspondence**
Balbir Singh Patial
Department of Physics, Himachal Pradesh University, Summerhill, Shimla, Himachal Pradesh-171005, India

Email: bspatial@gmail.com

How to cite this article
Monika, Ashish Kumar Mishra, Balbir Singh Patial, Sol-Gel Synthesis, Crystalline Size, Dislocation Density and Microstrain of $LiNi_{0.85}Co_{0.10}Mn_{0.05}O_2$ Cathode Material for Lithium-Ion Batteries, J. Cond. Matt. 2023; 01 (02): 65-68

Available from:
https://doi.org/10.61343/jcm.v1i02.46

Introduction

Lithium-ion batteries (LIBs) have undergone a transformative evolution, impacting diverse sectors through their remarkable attributes of high energy density and extended cycle life [1-2]. Central to the LIB architecture, the cathode wields considerable influence over battery performance. A pursuit of advanced cathode materials, those that can amplify capacity, stability and voltage traits, is underway with a particular spotlight on the synergistic Ni-Co-Mn (NCM) composition. This composite engenders have different characteristics that work well together [3-6], promising a paradigm shift in the trajectory of future LIBs. In the complex process of creating cathodes, the sol-gel technique has become widely recognized and important. This methodology offers a tailored approach, wielding precise control over material attributes. Our study embarks on an exploration of NCM cathode synthesis using the sol-gel method [7-9]. Through this, we unveil intricate structural insights, casting light on the latent potential of the synthesized cathode material for LIB application. In essence, this endeavor propels our understanding of cathode materials and their interplay with battery performance.

The prowess of Ni-rich cathodes resonates in their energy storage capabilities. $LiNi_xMn_yCo_{1-x-y}O_2$, where $x \geq 0.5$ (NCM) compositions hold the promise of elevated energy densities and extended battery life [10-11]. Notably, $LiNi_{0.85}Co_{0.10}Mn_{0.05}O_2$ embodies a deft equilibrium, harmonizing nickel's capacity, cobalt's structural robustness and manganese's prowess in controlling capacity fading [12]. This composition is primed to address inherent challenges faced by conventional cathode materials. However, the journey towards harnessing Ni-rich cathodes is not devoid of challenges. A notable concern is the structural instability and voltage attenuation experienced during cycling. The incorporation of a high nickel content often triggers phase transitions and structural deterioration,

culminating in the gradual decay of capacity over prolonged charge-discharge cycles [13-16]. Moreover, batteries with cathodes rich in nickel often encounter issues when they react with the electrolyte causing resistance to increase and cycling efficiency to decrease. To address these problems, researchers have been studied various methods. These include new ways of coating the cathode, carefully adding different materials and adjusting the proportions of the components. These efforts aim to improve the stability, cycling performance and safety of cathode materials with nickel.

This study helps us understand how different metals like nickel, cobalt, and manganese come together to create materials used in batteries, especially for electric cars. The study focused on a specific mix called $LiNi_{0.85}Co_{0.10}Mn_{0.05}O_2$ and how it's produced. Through this investigation, the study revealed both the positive aspects and challenges of using these materials. Overall, it contributes to advancing our ability to create battery components and guides us in making excellent batteries that can store a significant amount of energy, benefiting devices like laptops, electric cars, etc.

Experimental details

1. Material synthesis

The cathode material $LiNi_{0.85}Co_{0.10}Mn_{0.05}O_2$ (say M5) was synthesized through the application of the sol-gel method. Equimolar quantities of lithium nitrate, nickel nitrate hexahydrate, manganese acetate tetrahydrate and cobalt nitrate hexahydrate with 1:1 ratio, were dissolved in distilled water and blended with citric acid. The mixture was stirred for 8 h duration at room temperature. Following this, the solution underwent evaporation under continuous stirring at 80 °C until a thick green aqua-gel substance formed. After the drying process, the moist gel was held at 120 °C until it transformed into a xerogel. This xerogel was subsequently fragmented and subjected to a calcination process at 500 °C for 5 h within furnace. This step aimed to break down the organic components and nitrate constituents. Following the calcination, the sample was subjected to grinding, followed by sintering at 850 °C for a duration of 12 h in the furnace, without the formation of pellets. Upon reaching room temperature, the final product $LiNi_{0.85}Co_{0.10}Mn_{0.05}O_2$, was successfully obtained.

2. Material Characterization using X-ray Diffraction (XRD)

XRD serves as a guiding light, revealing the intricate structural nuances. Our rigorous examination of $LiNi_{0.85}Co_{0.10}Mn_{0.05}O_2$ utilized to conduct expansive scans across a broad $0° < 2\theta < 90°$. These scans unveiled diffraction patterns resembling celestial constellations, marking the coordinates of crystallographic peaks and the spaces between them, providing a direct window into the elaborate crystal arrangement of the material. Figure 1 shows the XRD pattern of investigated sample M5. Anchored by the Scherrer equation [17] ($D = 0.9\lambda / \beta \cos\theta$), where θ, peak full-width at half-maximum (β) was converted into radian and λ representing the X-ray wavelength, elegantly transitioned into the realm of nanometers. This meticulous translation unveiled crystallite sizes, unraveling a dual narrative of peak broadening and the dimensions of crystalline entities. This revelation enriched our understanding of how these dimensions interplay with peak broadening and the very essence of crystallites, lending depth to our comprehension of the material's core characteristics.

Table 1: Values of average crystallite size (D), dislocation density (δ), and strain (ε) for $LiNi_{0.85}Co_{0.10}Mn_{0.05}O_2$ nanocrystalline system.

Position of the peak (2θ)	FWHM	Crystallite Size (*D*) (nm)	Dislocation density ($\delta \times 10^{15}$ lines/ m^2)	Strain ($\varepsilon \times 10^{-3}$)
28.98	0.20	39.72	0.63	0.87
30.21	0.17	46.31	0.46	0.80
37.07	0.19	42.95	0.54	0.80
43.10	0.13	63.90	0.24	0.54
53.00	0.33	26.59	1.41	1.30
62.62	0.25	35.90	0.77	0.96
75.13	0.20	49.99	0.40	0.69
79.12	0.32	31.95	0.97	1.08

Results and Discussion

XRD analyses the sample M5 under investigation show distinct 2θ peaks (Table 1) with associated FWHM values. These FWHM variations indicate different crystalline traits and provide insights into potential uses. Scherrer equation calculations offer crystallite sizes (D) for the range of 26.59 nm to 63.90 nm. The number of defects and imperfections in crystal lattice can be provided by dislocation density of system and is calculated by using the relation [18]:

$$\delta = 1/D^2 \quad (1)$$

Moreover, microstrain (ε) developed owing to displacement of atoms with respect to their reference lattice position and determined by the following relation [19]:

$$\varepsilon = \beta \cos\theta / 4 \quad (2)$$

The deduced values of δ and ε are given in Table 1. Variation in crystallite size is observed. The intriguing variations in FWHM provide a glimpse into diverse crystalline attributes, suggesting a spectrum of potential applications.

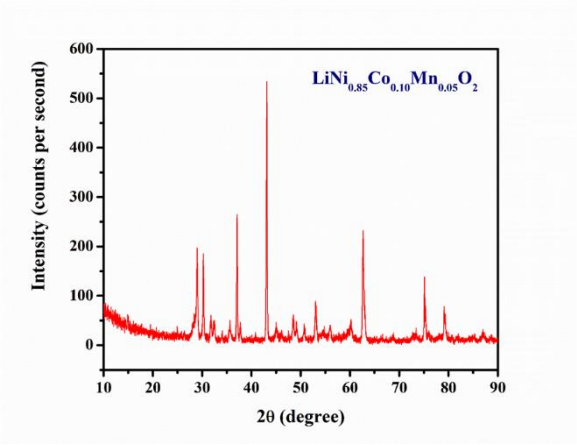

Figure 1: XRD pattern of $LiNi_{0.85}Co_{0.10}Mn_{0.05}O_2$ (NCM) cathode material

Conclusion

This paper uncovers the crucial role of crystalline size in shaping the performance of lithium-ion batteries. Smaller crystal sizes within cathode materials lead to notable benefits, such as a larger surface area that facilitates faster movement of lithium ions, resulting in improved charge and discharge rates. Moreover, these reduced crystal sizes contribute to less mechanical stress during battery operation, potentially extending the battery's overall lifespan. The use of X-ray analysis reveals distinct patterns for sample, underlining the varied crystalline characteristics. The calculated crystal sizes ranging from 26.59 nm to 63.90 nm highlight a remarkable diversity in particle sizes. Additionally, exploring dislocation density (δ) and micro-strain (ε) provides deeper insights into the materials' structural traits, with differing δ values indicating variations in structural integrity, and ε values reflecting a range of strains within the nanocrystalline structure. Collectively, these findings significantly advance our grasp of the structural properties of $LiNi_{0.85}Co_{0.10}Mn_{0.05}O_2$ nanocrystalline system. By deciphering the intricate relationships between crystallite size, dislocation density, and microstrain, this research offers valuable insights for tailoring these materials to specific applications, particularly in high-performance lithium-ion battery systems. The knowledge gained from this analysis not only deepens our understanding of nanocrystalline systems but also charts a path for their optimized integration into state-of-the-art energy storage solutions.

References

1. J Xie, and Y C Lu. Nature communications 11:2499, 2020.
2. C P Grey and D S Hall. Nature communications 11:6279, 2020.
3. W He, W Guo, H Wu, L Lin, Q Liu, X Han, Q Xie, P Liu, H Zheng, L Wang, X Yu and D L Peng. Advanced Materials 33:2005937, 2021.
4. M Kotal, S Jakhar, S Roy and H K Sharma Journal of Energy Storage 47:103534, 2022.
5. H H Ryu, B Kamboong, J K Kim, L Belharouak, C S Yoon and Y K Sun. ACS Energy Letters 6:2726-2734, 2021.
6. F K Geldasa, M A Kebede, M W Shura and F G Hone. RSC advances 12:5891-5909, 2022.
7. A E Danks, S R Hall and Z J Schnepp. Materials Horizons 3:91-112, 2016.
8. D Bokov, A T Jalil, S Chupradit, W Suksatan, M J Ansari, I H Shewael, G H Valiev and E Kianfan. Advances in Materials Science and Engineering 2021:1-21, 2021
9. X Wang. Vidyasirimedhi Inst. Sci. Technol 25:1-30, 2020.
10. L Hailong, X G Sun and S Dai. Advanced Energy and Sustainability Research 2:2000044, 2021.
11. J Xiang, Y Wei, Y Zhong, Y Yang, H Chang, L Yuan, H Xu and Y Huang. Advanced Materials 34:2200912, 2022.
12. X Ou, T Liu, W Zhong, X Fan, X Guo, X Haung, L cao, J H B Zhang, Y S Chu, G Hu, Z Lin, M Dahbi, J Alami, F Wu, K Amine, C Yang, J Dong and J Lu. Nature communications 13:2319,2022.
13. A Butt, G Ali, K T Kubra, R Sharif, A Salaman, M Bashir and S Jamil. Energy Technology 10: 2100775, 2022.
14. Z Xiao, P Liu, L Song, Z Cao, J Du and C Zhou. Ionics 27:3207-3217, 2021.

15. L Caijian, F Li, and J Liu. Nanomaterials 12:1888, 2022.
16. F Wu, J Dong, L Chen, L Bao, N Li, D Cao, Y Lu, R Xue, N Liu, L Wei, Z Wang, S Chen and Y Su. Energy Storage Materials 41:495-504, 2021.
17. A L Patterson. Physical review 56: 978, 1939.
18. R B Calhoun and D C Dunand. Comprehensive Composite Materials: Metal Matrix Composites.3:27-59, 2000.
19. Y Zhao and Z Jianzhong. Journal of Applied Crystallography 41:1095-1108, 2008.